Signal and Pattern Generation for Muscle Manipulation in Medical Applications

Hagit Perets Habany, *Student Member*, *IEEE*, Michael Evzelman, *Member*, *IEEE* and Mor Mordechai Peretz, *Member*, *IEEE*

The Center for Power Electronics and Mixed-Signal IC, Department of Electrical and Computer Engineering
Ben-Gurion University of the Negev, P.O. Box 653, Beer-Sheva, 8410501 Israel
hagitpe@post.bgu.ac.il, evzelman@bgu.ac.il, morp@bgu.ac.il
http://www.ee.bgu.ac.il/~pemic

***Abstract* — A sinusoidal power generator targeted to relax muscles associated with airway channel, and to assist in human intubation, is designed and implemented. The relaxation of the muscles needs to be achieved through external stimulation of the nerves, i.e. excitation of the nerves through the skin. The device is built around two-stage power system that include a DC-DC pre-regulation stage and sinusoidal waveform generator – series-resonant parallel-loaded converter. The unique, non-linear load characteristics of the human skin present a challenge for the converter to maintain the output current regulated. This is required to monitor the amount of charge that is transferred to the subject. To address the challenges, the converter is operated above the resonant frequency to facilitate current sourcing, and a pre-regulation stage is used to control the amplitude of the sinusoidal excitation current independent of the frequency. Load characteristics, control algorithm, converter operation, design challenges and critical considerations are discussed and validated experimentally on the proof of concept laboratory prototype.**

Keywords – Resonant Converter, Medical, Sinusoidal Generator, Current Source, HFAC

I. Introduction

Intubation in humans is a procedure that involves inserting tube into the trachea in order to maintain an open airway. In emergency cases once the breathing channel is closed, the common practice is to provide medication treatment to allow the channel opening. There are some major drawbacks associated with medication treatment such as delayed onset and offset operation, requirement of intravenous access, contraindications to use and side effects [1]-[3]. These limitations delay and prevent airway opening and in some cases can cause permanent neurologic injury, or death from hypoxia – oxygen deficiency in body tissues. Much better alternative would be to excite the nerves responsible for muscle relaxation and that will open the breathing channel. One way to excite the nerves would be using an electrical current (Fig. 1). One of the challenges associated with this approach is a non-linear impedance behavior of the skin. Before the conduction path through the skin is established, its impedance is about kilo ohm to several kilo ohms, but once the skin conducts, its impedance drops to hundreds of ohms [4]. Driving nonlinear load such as the body using current source requires a tight control of the current amplitude over a wide load range on the one hand, while on the other hand the right excitation frequency needs to be maintained to continue the excitation of the nerve. Previous literature covers several excitation methods and signal patterns to influence nerves, and while there are some studies that implement the power generators [5], [6], the approaches used are mostly linear, inefficient circuits that are large in size and power hungry. The objective of this study is to design and implement portable sinusoidal current generator with programmable application pattern, with low Total Harmonic Distortion (THD), capable to adjust and tightly follow output frequency and amplitude, creating unique signal patterns suitable to excite the nerves involved.

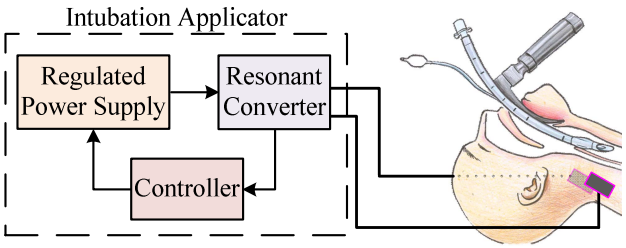

Fig. 1. Abstractive representation of the generator and the subject of application.

The rest of the paper is organized as follows: Section II presents the architecture of the system, principle of operation of the two-stage converter, sinusoidal current sensing approach, and control algorithm. Section III details practical implementation challenges. Section IV shows the experimental results of the two stage sinusoidal generator driving tissue-emulating loads, including step response changing from high impedance to low impedance loads. Section V concludes the paper.

II. Two Stage Current Sourcing Sinusoidal Generator

Generation of sinusoidal current waveforms can be implemented using a single resonant converter stage [7] – [13]. However, when driving a nonlinear load, such as the human body, through the skin and other tissues (Fig. 2a), there is a

challenge to maintain current amplitude as well as programmable frequency. In addition, current requirements to relax the muscle and to maintain it relaxed are not the same. Higher current is required to initiate muscle relaxation, but once muscle relaxation is induced, a much smaller amplitude current is required in order to maintain relaxation. To address this challenge, a functionality of programmable pattern generation, such as shown in Fig. 2b, is required. Additional requirements for the final product are isolation, which is required to address the safety issue, and total charge regulation to avoid damage to sensitive tissues.

To achieve sinusoidal current waveforms compliant with the goals outlined above, a two-stage topology is required [14] – [17]. The topology selected in this study consists of a first stage buck converter followed by a series-resonant parallel-loaded converter. The buck converter adjusts the input voltage to the second stage, whereas the second stage produces high frequency alternating current (HFAC). The resonant converter is in charge of generating the sinusoidal waveform at the target frequency with current sourcing attributes, while the first stage buck converter tunes the output current amplitude to meet the reference current and compensates the resonant tank gain variation over the frequency range of interest.

A. Series-Resonant Parallel-Loaded Converter

There are several resonant converter options suitable to generate sinusoidal waveforms with low THD [18]. The simplest and easiest for implementation is the series resonant converter. However, for the range of frequencies required to excite the nerve, a very high inductance is required to achieve reasonably high quality factor, Q (1) to maintain low THD, which in turn translates into a physically large inductor size. The topology of choice in this study is the series-resonant parallel-loaded converter [12], which has a higher quality factor, $Q_{parallel}$ than the quality factor of the series resonant circuit, Q_{serial} at larger resistances and so it is more suitable for the application.

$$Q_{parallel} = \frac{R_{load}}{Z_r}, Q_{serial} = \frac{Z_r}{R_{load}}, Z_r = \sqrt{\frac{L_{res}}{C_{res}}} \quad (1)$$

Series-resonant parallel-loaded converter operates by switching the half bridge switches S_H, S_L (Fig. 3) in a complementary manner driving the resonant network at the target frequency. The voltage V_x can be expressed using the Fourier series:

$$V_x = \frac{2V_{Buck}}{\pi} \cdot \sum_{n=1,3,5\ldots}^{\infty} \frac{1}{n} \sin(2\pi f_{sw} t) + \frac{V_{Buck}}{2} \quad (2)$$

When switching frequency f_{sw}, is in the vicinity of the resonant frequency f_{res}, $f_{res} \approx f_{sw}$, a first harmonic approximation can be applied and the half bridge inverter is described as a sinusoidal source connected to a series resonant network with a parallel load, as shown in Fig. 4 [19]. The voltage V_x can be simplified and expressed as:

$$V_x = \frac{2V_{Buck}}{\pi} \sin(2\pi f_{sw} t) + \frac{V_{Buck}}{2} \quad (3)$$

To avoid DC currents through the inductor, blocking capacitor C_s is used. For $C_s >> C_{res}$ the expression for output current according to the notations of Fig. 3 is:

$$I_{out} = \frac{2V_{Buck}}{\pi \cdot R_{load}} \cdot \frac{1}{1 + s\frac{L_{res}}{R_{load}} + s^2 L_{res} C_{res}} \quad (4)$$

where the resonant frequency f_{res} is:

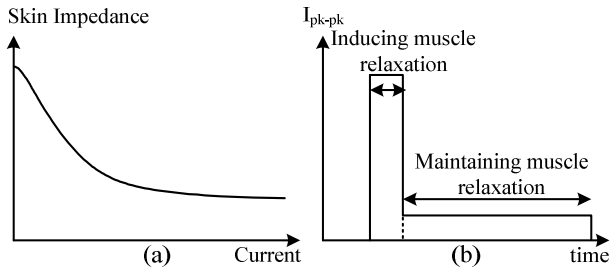

Fig. 2. (a) Skin impedance behavior, (b) Current pattern generation.

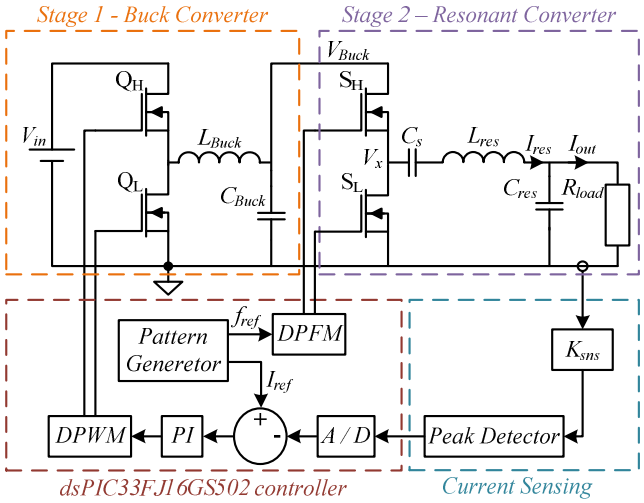

Fig. 3. Schematic of the power stage and control blocks.

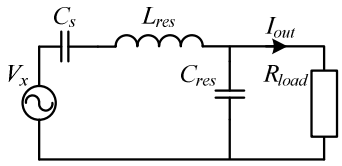

Fig. 4. An equivalent circuit of the resonant converter stage

$$f_{res} = \frac{1}{2\pi\sqrt{L_{res}C_{res}}} \quad (5)$$

It can be seen from (4) that the output current depends on both the input voltage V_{Buck} and the load R_{load}. Therefore, in order to maintain constant output current in the presence of load changes and fixed frequency, additional degree of freedom is required, such as the ability to change the input voltage to the resonant stage V_{Buck}.

B. Front-End Buck Converter

The function of the pre-regulation stage is to adjust the amplitude of the output current in the presence of wide load and input voltage variation. Input voltage variation could be due to the battery charge/discharge, while load variation comes from non-linear characteristics of the skin. Pre-regulation stage could be DC-DC converter to provide step-up, step-down or step-up/down options depending on the source, and desired operation range. Since the prototype developed in this study has been operated off a laboratory power supply, step down buck converter was selected. The impact of skin conduction on the

converter loading is shown in Fig. 2a. For the matter of response evaluation, skin-loading behavior could be approximately modeled as a step from high impedance to low impedance load. Step from high impedance to low impedance results in a rise of the load current amplitude.

One possible option to compensate the change in output current amplitude is to shift the switching frequency and change the gain of the resonant converter. This is however, prohibitive in the application where both THD and tight frequency control are required [20]. The alternative solution is to use pre-regulation stage to adjust the voltage fed to the resonant converter, which in turn adjusts the amplitude of the output current. PWM control is employed to adjust the output of the buck stage, and the control loop is designed to adjust the duty cycle of the buck stage as a function of the amplitude of the sinusoidal output current.

C. Current Sensing

One of the options to implement current sensing of an AC signal is using a current transformer. The benefit of the method comparing for example to a series-sense resistor,[21], is the efficiency. Current amplitudes required in this study are in the range of 1 mA to 30 mA. In order to facilitate good signal to noise ratio and to create an acceptable interface to the microcontroller's Analog to Digital Converter (ADC), the sensed current is passed through several gaining and shaping units (Fig. 5a).

First is the current transformer itself, which is designed with high transfer ratio, 1:100 in this work. Then the current at the secondary, I_{sns} is converted into voltage by flowing through resistor R_1 (Fig. 5b). It should be noted that although low current amplitudes are measured, a high attenuation current sensor is used. This is to facilitate reduced interference measurement with low power consumption. In addition, since the output current (rather than the resonant one) is the target of this application, it is desired to add minimal amount of additional parasitic inductance to the loop. Capacitor C_1 is used to smooth the voltage waveform. Next, a full wave rectifier built around operational amplifier both rectifies the sinusoidal signal and further amplifies it to match the dynamic level of MCU's built in ADC. Finally, to reduce the sampling rate requirements of the ADC, and reduce its power consumption, an analog peak detector is used. Peak detector is implemented around operational amplifier to allow compensation of the rectifying diode D_3 voltage drop. The time constant of the peak detector is selected approximately ten times the period of the sinusoidal waveform to both, filter out the ripple, and smoothly follow the sinus peak value. The amplifiers are fed with bipolar power supply to allow the negative input of the sinusoidal waveform. Alternatively, the potential of full wave rectifier reference and the secondary winding of the current transformer could be raised enough above the ground to allow unidirectional operation.

D. Control of a Two Stage Topology

The main control challenge in this study, associated with maintaining constant output current in the presence of wide non-linear load variation introduced mainly by the human skin (Fig. 2a). The best way to address it is by introducing an ideal sinusoidal current source. Resonant circuits could be treated as

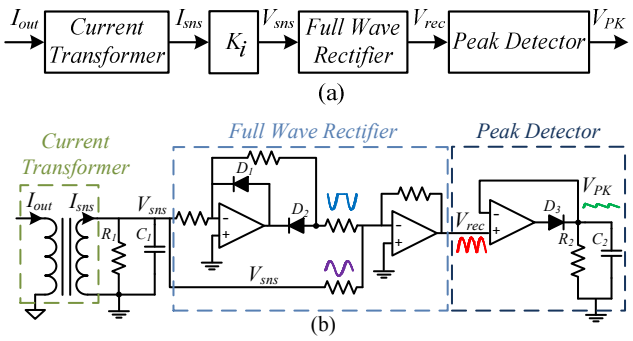

Fig. 5. Current sensing schematics diagram. (a) Block diagram (b) Circuit level schematics.

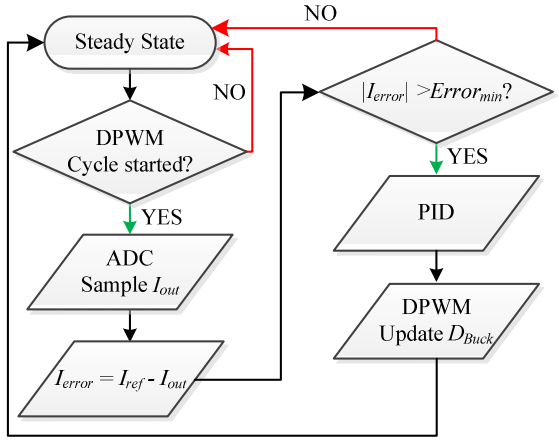

Fig. 6. Flow-Chart of the two-stage controller.

current sources in the immediate vicinity of their resonant frequency. However, it is unpractical in the real system due to very high quality factor required, which in turn poses another challenge of locking in the operation frequency close enough to the resonant frequency. Finally, if the operation frequency needs to be adjusted on demand, to maintain current source characteristics a continuously variable resonance component is required. An alternative to ideal current source would be a controlled system that is able to regulate the frequency and the output current amplitude independently. The user has an independent freedom to change the frequency of the second stage, by adjusting the switching frequency of the resonant converter, and to adjust the output current amplitude by regulating the voltage of the first stage (Fig. 3).

To address the control management requirements an MCU is used. Every cycle of the resonant stage, the output voltage of the peak detector V_{PK} is sampled by the ADC. Then, a calculation of the current error is preformed and if the error exceeds the maximum acceptable limit, a PID compensator calculates the new duty cycle D_{Buck}, which is then fed to the front-end stage. A flowchart of the algorithm is shown in Fig. 6. Additional MCU function is pattern generation. The references of frequency and amplitude provided to the controller by the pattern generation block (Fig. 3) are varied in time to achieve certain medical functionality. In the example shown in Fig. 2b, first muscle relaxation is induced with higher current for short

period, and then in order to hold the muscle relaxed, the current is significantly reduced and maintained for a longer period.

E. Safety

An important aspect of medical devices regards to safety concerns for both the subject and the applicator. To assure that current flows on to the subject alone within the confined region of the contact electrodes, i.e., there is no electrocution hazard to the applicator, the current flow needs to be governed and monitored on both electrodes. This can be facilitated using a single current transformer, occupying two turns on its primary, one turn from the signal line and the other from the return path. A zero-sum reading of the transformer assures that the entire current flows in the desired path without leakage. It should be noted that although isolation is used in the application, parasitic capacitance leakage is still feasible, and therefore an extra measure of caution needs to be employed. To satisfy the safety of the subject, and to prevent damage or burn of the sensitive tissues due to arching, the charge flow out of each electrode is continuously monitored, so that the application does not exceed the allowed per pulse as well as accumulative charge quantity.

III. Design Considerations and Practical Implementation

The load range of the converter is located in between 100 Ω to 10 kΩ [4]. The minimum quality factor, Q_{min} of the series-resonant parallel-loaded converter is selected according to the THD requirements. Very high quality factors however, are undesired either. High quality factor results in much higher reactive currents that circulate in the system and reducing system efficiency, steep transfer function that is challenging in terms of frequency and gain control. In addition, an underdamped system has long convergence time. Therefore, the upper limit for the quality factor is limited to around 100, while the minimum quality factor has been selected to be three. To maintain the minimum quality factor, the design of the converter is carried out for the worst-case conditions, i.e. the load resistance of 100 Ω. Operation of the converter is desirable in the inductive range, i.e. above the resonance frequency of the RLC network, which provides current sourcing behavior and enables ZVS of the main resonant converter switches, and as a result, lower losses are obtained. The target operation-frequency range in this study is set to 10 kHz – 40 kHz, which is the most prominent range for nerve manipulation according to the medical studies [22] - [25]. It is implemented using separate inductors, L_{res}, to achieve different resonant frequencies. The resonant frequency of the series resonant tank is selected slightly lower than the lowest expected operation frequency. Using (1), (5) and the considerations of the resonant frequency and quality factor outlined above the values of L_{res} and C_{res} are selected according to:

$$C_{res} = \frac{Q}{2\pi f_{res} R_{load}}\ , L_{res} = \frac{1}{C_{res}(2\pi f_{res})^2} \tag{6}$$

Resonant inductor is designed for the worst-case conditions, which is the highest expected current in the circuit. The inductor in this circuit configuration carries larger current than the current provided to the load. The ratio between the output current I_{out} and the resonant inductor current I_{res} could be summarized in the following expression:

$$\frac{I_{out}}{I_{res}} = \left| \frac{1}{1 + j\cdot(2\pi f_{sw}) C_{res} R_{load}} \right| . \tag{7}$$

Rearranging (7) and substituting C_{res} from (6), resonant current can be expressed as:

$$I_{res} = I_{out} \cdot \sqrt{1 + \left(\frac{f_{sw}}{f_{res}} \cdot Q\right)^2} \tag{8}$$

It follows from (8) that the worst-case conditions for resonant inductor, in terms of maximum resonant current, occur at the highest quality factor. This conclusion holds assuming the rest of the parameters are kept constant, such as the output current that is maintained constant by the buck converter, and switching frequency that is set according to the medical specifications.

To avoid DC offsets associated with parallel loading of the series resonant circuit fed off a half bridge, a blocking capacitor C_s is used. Blocking capacitor C_s, is selected to be large enough comparing to the resonant capacitor C_{res}, to minimize the ripple and maintain the voltage constant.

IV. Experimental Verification

To validate the design presented in this study a laboratory prototype of a two stage resonant sinusoidal generator has been designed and built. The converter is digitally controlled by a dsPIC33FJ16GS502 microcontroller manufactured by Microchip [26]. The parameters of the system are summarized in Table I. Converter operation is shown in Fig. 7. Sinusoidal current waveform with low distortion is shown in Fig. 7a. The FFT transformation of I_{out} is shown in Fig. 7b. The THD of the waveform in Fig. 7b has been calculated based on the FFT values, and found to be 2%.

The system's response to load changes is demonstrated in Fig. 8. A step from light load 1 kΩ to heavy load 100 Ω, i.e. the condition of high initial resistance of the skin that is reduced after the conduction is initiated is shown in Fig. 8a. The system adjusts to the reference output current in less than 2 ms, which is approximately 30 switching cycles of 14 kHz sinusoidal waveform, and is approximately the quality factor of the circuit at these conditions. An opposite step from heavy load of 100 Ω to the light load of 1 kΩ is shown in Fig. 8b. Current pattern generation capability is shown in Fig. 8Fig. 9. Current pattern that was discussed in Fig. 2b that requires higher current for short period to induce muscle relaxation, and then much lower current to maintain muscle relaxation is shown in Fig. 9a, repeated at 6Hz. Additional pattern with three different amplitudes and time periods is shown in Fig. 9b.

TABLE I – Two stage system parameters

Component	*Value / Type*
Input voltage V_{in}	22V
Load resistance range	100 – 10000 Ω
Output voltage V_{out}	10V - 300V pk-pk
Frequency range f_{ref}	10 kHz - 40 kHz
Resonant capacitor C_{res}	150 nF
Resonant inductor L_{res}	2 mH / 180µH
Blocking capacitor C_s	1.1 µF

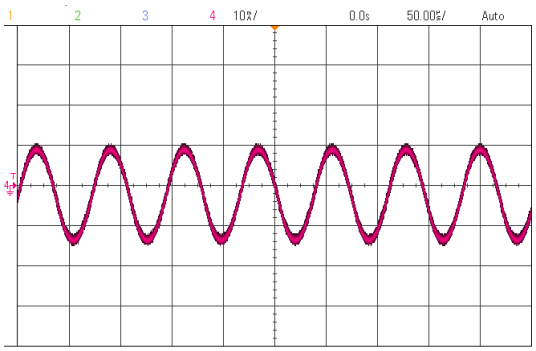

(a)

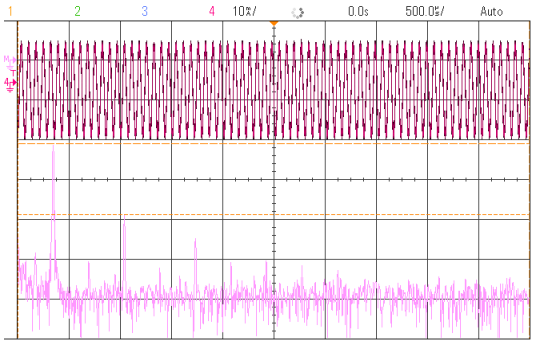

(b)

Fig. 7. Converter operation: (a) Time domain sinusoidal output current, I_{out} (10mA/div), Horizontal axis (50us/div); (b) FFT of the output current, Top trace (red) – Output current I_{out} (10mA/div), Horizontal axis (500us/div); Bottom trace (pink) – FFT of the output current (20dB/div), Horizontal axis (20kHz/div);

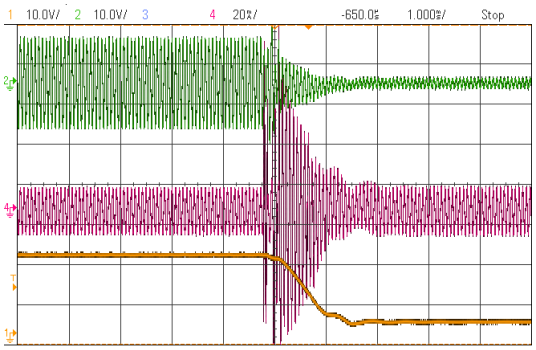

(a)

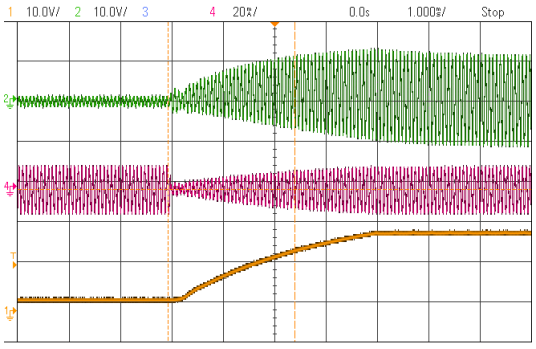

(b)

Fig. 8. Load change compensation: (a) 1000[Ω] to 100[Ω]. (b) 100[Ω] to 1000[Ω]. Top trace (green) – Output voltage V_{out} (10V/div). Middle trace (red)

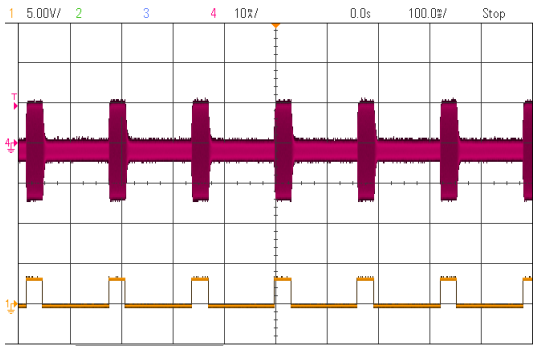

(a)

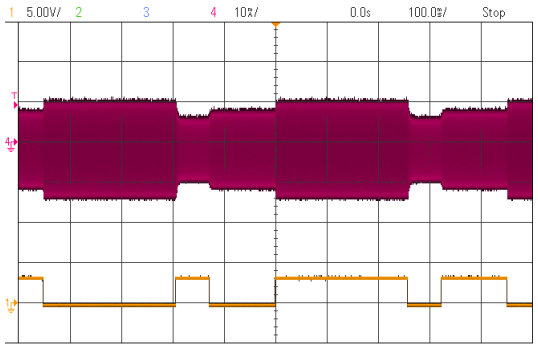

(b)

Fig. 9. Pattern generation - changing current amplitude. Top trace (red) – Output current I_{out} (10mA/div). Bottom trace (yellow) – pattern synchronization signal.

An experiment with a non-linear load, bringing the load behavior as close as possible to the behavior of the skin and tissues around the neck was carried out. For this purpose a pattern of pulse bursts, where the pulse output is toggled between on and off state was generated, and the load was varied from burst to burst. Load variation was carried out by initially connecting a 10kΩ resistor to the output, and then one of the experimenters was touching with his hand the application electrodes, connected to the output in parallel to the resistor Fig. 10. The resulting non-linear change in total resistance of the load could be tracked by the system response in Fig. 11. In Fig. 11a an experiment with a decrease in the output resistance is shown, i.e. the experimenter is touching the electrodes approximately after 3 horizontal divisions (at 60ms). As a result, buck output voltage (green trace) and the amplitude of the output voltage (yellow/brown trace) begin to decrease, while the amplitude of the output current is maintained constant, within the bandwidth limitations of the controller. In Fig. 11b an experiment with an increase in the output resistance is shown, where the experimenter holds the electrodes at the beginning, and releases them at approximately 100-110ms.

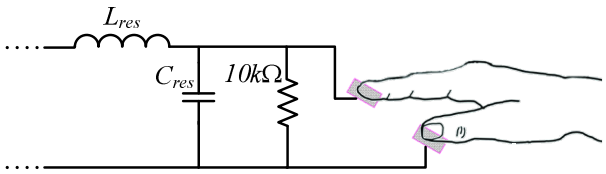

Fig. 10. Experimental setup for non-linear load change.

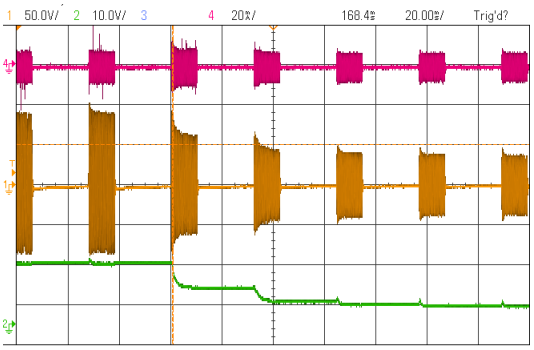

(a)

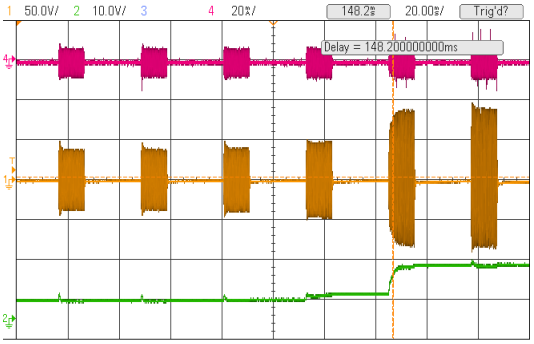

(b)

Fig. 11. Non-linear load change during burst generation. (a) Load increase (resistance decrease); (b) Load decrease (resistance increase).

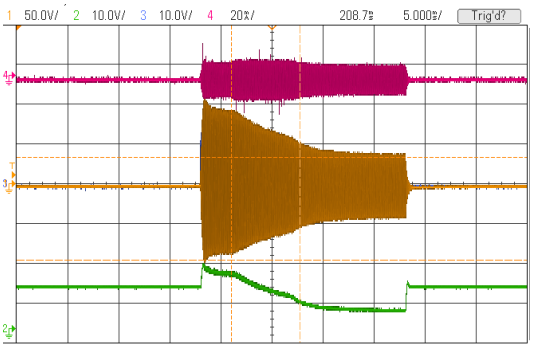

Fig. 12. Non-linear load change during a single burst of pulses. Load increased and resistance decreased.

As a result, buck output voltage (green trace) and the amplitude of the output voltage (yellow/brown trace) begin to increase. As in the previous case the amplitude of the output current is maintained constant by the system, achieving a behavior of nearly ideal current source.

To evaluate the system response to non-linear load application during a single burst of pulses, a 20ms burst was generated, and an experimenter touching of the electrodes was timed to coincide with approximately the beginning of the burst. The resulting system response is shown in Fig. 12. It can be seen that during the first 10ms after the beginning of the pulses burst, and the application of the non-linear load, the system carries out a series of corrections to maintain the current constant. Despite a slight increase in the output current as a response to the load, which is due to the limitations of the controller bandwidth, overall current amplitude is maintained very close to the reference value during the load variation period. Another observation from Fig. 12 is the non-linear practical response of the skin and the tissue, which is due to the constant current maintained by the system, could be derived from the buck output voltage (green trace).

V. Conclusion

A two stage sinusoidal current generator for muscle manipulation over the skin has been presented. High THD along with independent frequency and amplitude generation is achieved. The generator is capable to generate continuous current patterns tightly following the reference values in a presence of non-linear load, the skin in this case. Converter implementation is presented, control and current sensing approach is shown, design and implementation challenges along with their solutions are discussed. The requirements and challenges associated with assisting in human intubation i.e. target medical application are presented. The system was validated experimentally, running a series of experiments, including non-linear loads, and found to be in a good agreement with expected behavior.

VI. Acknowledgment

The authors would like to thank Dr. David Buck of CCHMC, who co-devised (together with Prof. Peretz) the original idea for airway muscle manipulation, for his contribution in this work, insightful comments that helped improve the prototype.

References

[1] R.C Sinclair and M.C Luxton, “Rapid sequence induction,” *Continuing Education in Anaesthesia Critical Care & Pain*, vol. 5, issue 2, pp. 45-48, 2005.

[2] G. Kovacs and J. A. Law, *Airway management in emergencies*, PMPH-USA, 2011.

[3] A. A. Alalami, C. M. Ayoub, and A. S. Baraka, “Laryngospasm: review of different prevention and treatment modalities,” *Pediatric Anesthesia*, vol.18, issue 4, pp. 281-288, 2008.

[4] Reilly, J. Patrick, *Applied bioelectricity: from electrical stimulation to electropathology*, Springer Science & Business Media, 2012.

[5] A. Rapeaux, E. Brunton, K. Nazarpour, and T. Constandinou, “Recovery Dynamics of the High Frequency Alternating Current Nerve Block,” 2017. Available: https://www.biorxiv.org/ [Accessed: July 2, 2018].

[6] R. P. Williamson and B. J. Andrews, "Localized electrical nerve blocking," *IEEE Transactions on Biomedical Engineering*, vol. 52, no. 3, pp. 362-370, March 2005.

[7] J. Hong, D. M. Vilathgamuwa, N. Ghasemi, T. Ishrat, and J. You, "A single phase DC-AC dual active bridge series resonant converter for photovoltaic applications," *IEEE 12th International Conference on Power Electronics and Drive Systems (PEDS)*, pp. 881-886, Honolulu, HI, 2017.

[8] Y. Jang and M. M. Jovanovic, "Constant-frequency resonant inverter for AC-bus distribution system," *Twentieth Annual IEEE Applied Power Electronics Conference and Exposition. APEC 2005*, Austin, TX, 2005, pp. 864-870 Vol. 2.

[9] Y. A. Ang, D. Stone, C. Bingham and M. Foster, "Rapid Analysis & Design Methodologies of High-Frequency LCLC Resonant Inverter as Electrodeless Fluorescent Lamp Ballast," *2007 IEEE 7th International Conference on Power Electronics and Drive Systems*, Bangkok, pp. 139-144, 2007.

[10] H. L. Li, A. Hu and G. A. Covic, "Development of a discrete energy injection inverter for contactless power transfer," *3rd IEEE Conference on Industrial Electronics and Applications*, Singapore, pp. 1757-1761, 2008.

[11] B. Dobrucky, M. Prazenica, S. Kascak and J. Kassa, "HF link LCTLC resonant converter with LF AC output," 38th Annual Conference on IEEE Industrial Electronics Society, Montreal, QC, pp. 447-452, 2012.

[12] S. Ben-Yaakov, M. M. Peretz, J. M. Parra, and J. M. Parra, "Self-Oscillating Constant-Current Fluorescent Lamp Driver: Theory and Application," *IEEE Power Electronics Specialists Conference*, Orlando, FL, pp. 3093-3099, 2007.

[13] G. C. Hsieh and C. M. Wang, "One-cycle controlled half-bridge series-resonant DC to AC inverter with reduced conduction loss," *IEEE Industrial Electronics, Control and Instrumentation*, 1997.23rd International Conference on, New Orleans, LA, vol.2, pp. 786-791, 1997.

[14] M. Evzelman, H. Wang, R. Zane and X. Zhao, "Two-stage sinusoidal generator with calibration and pulse train amplitude feedback for ultrasonic applications," *2017 IEEE Applied Power Electronics Conference and Exposition (APEC)*, Tampa, FL, pp. 2124-2130, 2017.

[15] F. J. Ferrero, M. Rico, J. M. Alonso, C. Blanco, M. Gonzalez and J. C. Campo, "A unity power factor electronic ballast for HPS lamps, resonant current controlled," *Conference Record of 1998 IEEE Industry Applications Conference. Thirty-Third IAS Annual Meeting*, St. Louis, MO, USA, vol.3, pp. 2122-2129, 1998.

[16] J. M. Correa, E. D. Hutto, F. A. Farret and M. G. Simoes, "A fuzzy-controlled pulse density modulation strategy for a series resonant inverter with wide load range," *Power Electronics Specialist Conference*, 2003. PESC '03. IEEE 34th Annual, vol.4, pp. 1650-1655, 2003.

[17] M. N. Kim, Y. S. Noh, J. G. Kim, T. W. Lee and C. Y. Won, "A new active power decoupling using Bi-directional Resonant Converter for flyback-type AC-module system," *2012 IEEE Vehicle Power and Propulsion Conference*, Seoul, pp. 1333-1337, 2012.

[18] R. L. Steigerwald, "A comparison of half-bridge resonant converter topologies," *IEEE Applied Power Electronics Conference and Exposition*, pp. 135-144, San Diego, CA USA, 1987.

[19] T. Duerbaum, "First harmonic approximation including design constraints," *INTELEC - Twentieth International Telecommunications Energy Conference (Cat. No.98CH36263)*, San Francisco, CA, USA, 1998, pp. 321-328.

[20] K. L. Kilgore and N. Bhadra. "Reversible nerve conduction block using kilohertz frequency alternating current," *Neuromodulation: Technology at the Neural Interface*, vol.17, issue 3, pp. 242-255, 2014.

[21] H. P. Forghani-zadeh and G. A. Rincon-Mora, "Current-sensing techniques for DC-DC converters," *2002 IEEE 45th Midwest Symposium on Circuits and Systems (MWSCAS)*, vol. 2, pp. 577-580, 2002.

[22] N. Bhadra, N. Bhadra, K. Kilgore, and K. Gustafson, "High frequency electrical conduction block of the pudendal nerve," *Journal of Neural Engineering,* vol. 3, num. 2, pp. 180-187, 2006.

[23] Kilgore, Kevin L., and N. Bhadra. "Nerve conduction block utilising high-frequency alternating current." *Medical and Biological Engineering and Computing*, vol. 3, issue. 42 pp. 394-406, 2004.

[24] N. Bhadra, E. Foldes, T. Vrabec, K. Kilgore, and N. Bhadra, "Temporary persistence of conduction block after prolonged kilohertz frequency alternating current on rat sciatic nerve," *Journal of neural engineering*, vol. 15, num. 1, 2018.

[25] Y. A. Patel, and R. J. Butera, "Differential fiber-specific block of nerve conduction in mammalian peripheral nerves using kilohertz electrical stimulation," *Journal of neurophysiology*, vol. 113, issue 10, pp. 3923-3929, 2015.

[26] Microchip Technology, Inc., "16-bit digital signal controllers with high speed PWM, ADC, and comparators," DS70000318G datasheet, 2008. [Revised May 2014].